

Characterizing Normal and Abnormal Cardiac Echo Motion Patterns

T Syeda-Mahmood¹, J Yang²

¹IBM Almaden Research Center, San Jose, CA, USA

²Siemens Corporate Research, Princeton, NJ, USA

Abstract

The Information about cardiac mechanical performance is of critical importance in understanding the etiology of heart diseases. However, little work has been done to date, to understand the relationship of cardiovascular diseases to the global cardiac motion patterns. In this paper we address the problem of distinguishing between normal and abnormal motion patterns in cardiac echo videos. Specifically, we describe the overall motion of the heart using average velocity curves. We then detect characteristic patterns in these curves that help distinguish normal from abnormal motion. The motion patterns observed in normal and abnormal groups using the extracted features are found to be easily separable.

1. Introduction

The Information about cardiac mechanical performance is of critical importance in understanding the etiology of heart diseases. However, little work has been done to date, to understand the relationship of cardiovascular diseases to the global cardiac motion patterns. Specifically, quantitative measures of describing motion patterns to more easily separate normal from abnormal cardiac echo motion are lacking.

Discerning motion abnormalities such as when the myocardium doesn't contract or contracts significantly less than the rest of the tissue, is difficult, in general for humans. Unlike the interpretation of static images such as X-rays, it is harder to describe the nature of the abnormalities in moving tissues. Physicians often resort to describing motion abnormalities using qualitative terms such as 'irregular motion', 'decay towards the end of a heart beat', or 'the twist is not firm enough', etc.

In this paper, we present a quantitative measure of describing motion patterns so as to more easily separate normal from abnormal cardiac echo motion. Distinguishing between normal and abnormal cardiac echo motion is easier than characterizing the nature of the abnormality (eg. Mitral valve prolapse), but is often the

first step whose automation can considerably shorten the time and costs associated with a diagnosis.

While there is considerable work in segmentation, tracking and estimation of cardiac wall motion [1-5], relatively little work has been done to date to understand the relationship of cardiovascular diseases to the global cardiac motion pattern.

2. Describing cardiac motion

Cardiac motion has a very complicated 3D non-rigid motion pattern. It involves twist, rotation, and contraction, which make it very difficult to describe all its characteristics through common feature extraction mechanisms. To model the truly non-rigid nature of cardiac motion, therefore, we utilize a representation of actions proposed earlier called the action cylinder [4]. The action cylinder was shown to be a robust representation of general actions of rigid, articulated and completely non-rigid motion, such as flowers moving in the wind [6]. To extract motion information from echo videos, we specifically focus on the axis of the cylinder and approximate it by an average velocity curve [4]. The average velocity curve is a temporal trajectory derived from successive instantaneous changes in direction and extent of average velocity. It is obtained by averaging the optical flow per frame. If we denote the intensity by $I(x,y,t)$, the spatio-temporal variation of brightness patterns is given by the brightness change constraint equation as

$$uI_x + vI_y = -I_t \quad (1)$$

where (I_x, I_y) are the partial derivatives of I , and u and v are the x and y components of the optical flow vector.

Assume the optical flow in an object region O in frame k be represented by the vectors $(U_k, V_k) = (u_{ij}, v_{ij}), i = 1, 2, \dots, M, j = 1, 2, \dots, N$, where (u_{ij}, v_{ij}) are the velocity vectors per pixel (i, j) within O in frame k . Then the average velocity vector for O in frame k is given by $(\delta_{avg}, \theta_{avg})$, where

$$\delta_{avg} = \frac{\sum_i \sum_j \sqrt{u_{ij}^2 + v_{ij}^2}}{MN}, \theta_{avg} = \frac{\sum_i \sum_j \tan^{-1} \frac{v_{ij}}{u_{ij}}}{MN} \quad (2)$$

For a 2-D image sequence, the spatio-temporal velocity curve is a curve in 3-D (2-D space + time) formed from successive average velocity vectors. Using a parametric representation based on time, the curve can be represented as a set of 2-D points $C(t) = (x(t), y(t)), k = 0, 1, \dots, T-1$ for a sequence of length T where

$$x(t+1) = x(t) + \delta_{avg} \cos(\theta_{avg}), y(t+1) = y(t) + \delta_{avg} \sin(\theta_{avg})$$

with $(x(0), y(0)) = (0, 0)$. (3)

Figure 1b illustrates the 3D average velocity curve for a cardiac echo video of a patient depicting Lateral Ventricular Global Hypokinesia shown in Figure 1a. The $X = \{x(t)\}$ and $Y = \{y(t)\}$ are components shown in Equation 3 and the time t is represented in terms of video frames. Here, the tracking of object began at frame 5. This plot represents average motion within a single heartbeat..

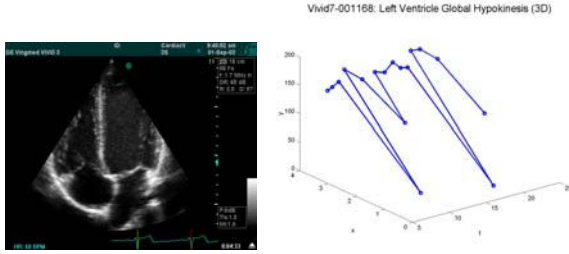


Figure 1: Illustration of feature extraction from cardiac echo videos. (a) Cardiac echo video snapshot. (b) Average velocity curve derived from the corresponding video.

To extract the average velocity curve, we compute motion in successive frames by subtracting intensity at identical locations in frames that are n apart (where we experimented with choice of n=5 or 10, i.e. frames that are 5 or 10 apart). This usually gets rid of the static portions such as text overlays and other markers in the video, leaving mostly the heart motion except from some noise in the image. Since the dominant object is always going to be the heart against a still background, this process also segments the object from the background so that the average velocity computations given by Equations 2 and 3 reflect the motion of the heart.

2.1. Extracting features from AVC

On examining the average velocity curves for various diseases as shown in Figure 2, it was observed that the average velocity curves of normal cardiac motions are more evenly distributed around a mean velocity. This is consistent with normal wall motion. Similarly, we

observed that a lack of sharp peaks in the average velocity curves, can be an indicator of abnormal cardiac motion. Thus a ratio of flat peaks to the original number of peaks can serve as a reliable feature to help distinguish between cardiac echo videos.

Let the time-average of X and Y component of AVC be denoted by M_X and M_Y respectively. Let

$$X_+ = \{X(t) | X(t) \geq M_X\}, X_- = \{X(t) | X(t) \leq M_X\} \quad (4)$$

Thus X_+ and X_- represent the number of velocity values that are above and below the mean velocity respectively. Similar measure can be defined for the Y component of average velocity. Then the average velocity distribution ratio is given by

$$V_{avg} = \frac{1}{2} \left(\frac{|X_+|}{|X_-|} + \frac{|Y_+|}{|Y_-|} \right) \quad (5)$$

To measure the fraction of flat peaks in the average velocity curve, we record the number of peaks that are within a threshold of the maximum height of a peak (depth of a valley) in the average velocity curve Δ_{max} as

$$F_X = \left\{ x(t) \mid \frac{\partial x}{\partial t} = 0, |x(t) - x(t-1)| < 0.125 \Delta_{max} \right. \\ \left. OR |x(t) - x(t+1)| < 0.125 \Delta_{max} \right\} \quad (6)$$

F_Y can be defined similarly. Then the flat peak ratio is given by

$$F_{avg} = \frac{1}{2N} (|F_X| + |F_Y|) \quad (7)$$

where N is the number of time samples available.

The features we extracted from AVC themselves have several advantages. First, since the average velocity distribution ratio and the flat peak ratio are normalized with respect to the samples, they are independent of the heart rate. So patient data reflecting fast or slow heart beats can be still be retrieved in a uniform way. Similarly, since they are normalized with respect to time units, they are invariant to the number of heart beats over which the videos were recorded. This is particularly important since a number of videos we tested had variable number of heart beats and these could be processed unaffected without segmentation of the videos per heart beat.

Since AVCs record projected motion, they are affected by changes in viewpoint. Hence the feature values are different for the same disease under long and short axis views. Figure 2 shows feature distribution of one of the data sets we experimented with that consisted of multiple videos corresponding to the same disease taken from different patients and using different view points (long In general though, this is not a problem, since only a small number of fixed viewpoints are used to collect the cardiac echo data. Also, such metadata is often supplied along with the diagnostic imaging equipment setting information. Within given viewpoints, however, the

average distribution of velocity distribution and flat peak ratios remain stable features to retrieve matching heart motion.

2.2. Separating normal/abnormal motion

Let $(V_{1avg}, F_{1avg}), (V_{2avg}, F_{2avg})$ be the feature vectors from two cardiac echo videos V1 and V2. Then the distance between the videos is given by the Euclidean distance as;

$$D(V_1, V_2) = \sqrt{(V_{1avg} - V_{2avg})^2 + (F_{1avg} - F_{2avg})^2} \quad (8)$$

Thus smaller values of distance indicate similar videos with identical videos receiving a 0.0 distance score. This distance measure can now be used to cluster normal and abnormal motion patterns.

Using the above features as a two-dimensional space, the cardiac echo videos of normal and abnormal heart motion can be easily clustered into two categories. We used a simple binary clustering algorithm to separate the clusters. Given any new sample data, we extract its average velocity curve and compute the same features. These are then projected into the clustering space and classified using a conventional classification algorithm such as a linear classifier.

3. Results

To verify the results of our conjecture that the average velocity curve and features extracted from it can serve as a robust classifier, we experimented with a number of cardiac echo data sets. In general, due to privacy concerns, the data sets for medical imaging are carefully guarded so that only limited data sets are available for public experimentation. Among the public data we used were three authentic reference sources, namely, the GE Vivid online medical library

(<http://vividlibrary.com>),

the trans-esophagus echo (TEE) video collection for Dr. Marty London at UCSF:

(<http://www.ucsf.edu/teeecho/>),

training videos on heart diseases from Yale Medical School

(http://info.med.yale.edu/intmed/cardio/echo_atlas/contents/index.html),

and congenital heart diseases collection from Yale (http://info.med.yale.edu/intmed/cardio/chd/e_as/index.html).

The data sets depicted over 500 cardiac echo videos from over 40 cardiac diseases; some are listed in Table 1.

For each disease, we had one or more views such as long axis, short axis, TEE etc. As some of the videos depicted multiple heart beat segments, we manually segmented the videos at multiples of heart beats to augment the data sets so that the combined collection

consisted of over 532 cardiac echo videos. The unsegmented videos were also made part of the collection to test invariance of features to duration of videos.

Sample diseases	Sample viewpoints
Pericardial effusion	Apical 4-chamber
Bicuspid disorder	Short-axis views
Mitral valve prolapse	Long axis views
Cardiomyopathy	Aortic short-axis
Normal (no disease)	
Abnormal Akinesis	
LV Lateral Basal Hypokinesis	
LV Concentric Hypertrophy	
Aortic Stenosis	
Mitral insufficiency	

Table 1: Illustration of diseases studied for cardiac motion patterns.

3.1 Discriminability of features

To show that the features extracted from average velocity curves can discriminate between normal and diseased heart motion, we recorded the values of the average velocity distribution ratio and the flat peak ratio for normal and diseased heart motion samples for the videos tested. The results for 12 of the videos from the GE Medical library collection show that the average ratios for normal subjects are around 1.0 and are much lower compared to that of the abnormal subjects for the average velocity distribution ratio. Similarly, the average percentages of the X and Y projections for normal and abnormal groups are quite different, where the normal ones have a very small percentage of flat peaks (less than 20-25%), but the abnormal subjects tend to have higher percentage, (more than 29%). Thus the features chosen provide sufficient discriminability to separate normal from abnormal motion.

Figure 2 shows the average velocity curves used for the feature computations. The underlying videos have been collected from different viewpoints (four chamber view, short axis view and long axis view, etc.) as well as patients with different heart rate and heart sizes. But the ranges of values of the features are relatively unaffected by the choice of viewpoint and heart rate specifics of individuals.

3.2. Classification accuracy

Of the 532 training videos, 387 pre-labeled training videos were used to form the clusters. The remaining data was using for testing the classification accuracy. Specifically, we tested the system with 145 query videos depicting different diseases and taken under different view points including long axis, short axis, 4-chamber,

TEE, etc. Of the 145 videos tested, 130 of them could be classified accurately. Thus the majority of the cardiac echo videos can be easily discriminated based on velocity distribution and flat peak ratios. Figure 3 shows the grouping for the GE vivid library collection. The data sets are easily separable in the feature space as shown in Figure 3.

The classification errors were skewed in favor of normal versus abnormal for some data sets. On analyzing the associated videos, it was found that such videos demonstrated other abnormalities besides motion abnormalities. Not surprisingly, anatomical abnormalities that manifest as size and shape differences of the region without affecting the motion pattern were classified incorrectly by the system.

4. Discussion and conclusions

In general, the misclassifications found were attributed to two reasons (a) when the features used for classification were insufficient, This is particularly the case for diseases related to shape abnormalities rather than motion abnormalities. (b) when motion involved regional motion that is not accurately represented by a single average velocity curve for the entire heart motion. In this case, it is possible to use pre-segmentation and apply the average velocity curve analysis locally to selected regions to more accurately reflect regional motion characteristics.

Overall, we found that the majority of cardiac diseases due to motion abnormalities could be easily characterized and separated from normal cardiac echo videos based on the simple features derived from average velocity curve described above.

References

- [1] Montillo A, Metaxas D, Axel L. Automated model-based segmentation of the left and right ventricles in tagged cardiac MRI. MICCAI (1) 2003: 507-515.
- [2] Papademetris X, Sinusas A, Dione D, Duncan J. 3D cardiac deformation from ultrasound images. In: Medical Image Computing and Computer Aided Intervention (MICCAI), (Cambridge, England) 1999: 420-429.
- [3] Zerhouni E, Parish D, Rogers W, Yang A, Shapiro E.. Human heart: tagging with MR imaging - a method for noninvasive assessment of myocardial motion. Radiology 1988; 169: 59-63.
- [4] Syeda-Mahmood T. Segmenting actions in velocity curve space. ICPR02 2002: 170-175.
- [5] Tagare H. Shape-based non-rigid curve correspondence with application to heart motion analysis. IEEE Transactions on Medical Imaging 1999; 18: 570-579.
- [6] Syeda-Mahmood T et al. Recognizing action events from multiple view points. Proc IEEE Workshop on detection and recognition of events in video (Vancouver) 2001.

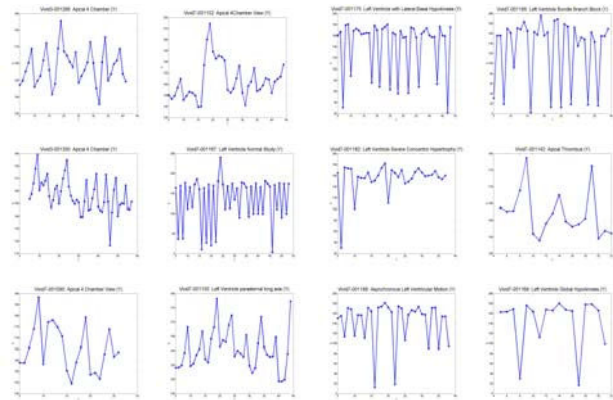


Figure 2. Illustration of average velocity curve projections (X and Y) for different diseased and healthy heart motion cases. Source: GE Vivid-online library.

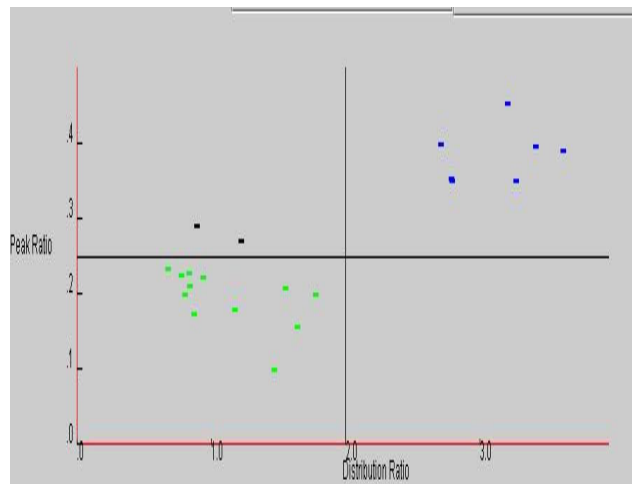


Figure 3: Illustration of separation of normal and abnormal echo videos for the GE Vivid collection.